Repurposing of anisomycin and oleandomycin as a potential anti-(SARS-CoV-2) virus targeting key enzymes using virtual computational approaches

Rafat Zrieq[1*], Mejdi Snoussi[2,3], Fahad D. Alqahtan[1,4], Munazzah Tasleem[5], Mohd Saeed[1], Emira Noumi[2,6], Nasrin E. Khalifa[7,8], Mohamed A. M. Gad-Elkareem[9], Kaïss Aouadi[10,11], Adel Kadri[12,13]

[1]Department of Public Health, College of Public Health and Health Informatics, University of Ha'il, Ha'il, Kingdom of Saudi Arabia
[2]Department of Biology, College of Science, Hail, P.O. 2440, University of Ha'il City 2440, Saudi Arabia
[3]Laboratory of Genetics, Biodiversity and Valorization of Bio-resources (LR11ES41), University of Monastir, Higher Institute of Biotechnology of Monastir, Avenue Tahar Haddad, BP74, 5000 Monastir, Tunisia
[4]Molecular Diagnostics and Personalised Therapeutics Unit, University of Ha'il, Ha'il, Kingdom of Saudi Arabia
[5]School of Electronic Science and Engineering, University of Electronic Science and Technology of China, Chengdu 610054, Sichuan, China
[6]Laboratory of Bioresources: Integrative Biology and Valorization, (LR14-ES06), University of Monastir, Monastir 5000, Tunisia
[7]Department of Pharmaceutics, College of Pharmacy, University of Hail, Kingdom of Saudi Arabia
[8]Department of Pharmaceutics, Faculty of Pharmacy, University of Khartoum, Sudan
[9]Department of Chemistry, Faculty of Science, Al-Azhar University, Assiut 71524, Egypt
[10]Department of Chemistry, College of Science, Qassim University, Buraidah 51452, Saudi Arabia
[11]University of Monastir, Faculty of Science of Monastir, Avenue of the Environment, 5019 Monastir, Tunisia
[12]Department of Chemistry, Faculty of Science and Arts of Baljurashi, Albaha University, Saudi Arabia
[13]Faculty of Science of Sfax, Department of Chemistry, University of Sfax, B.P. 1171, 3000 Sfax, Tunisia

ARTICLE INFO

ABSTRACT

Despite the accelerated emerging of vaccines, development against the severe acute respiratory syndrome coronavirus 2 (SARS CoV-2) drugs discovery is still in demand. Repurposing the existing drugs is an ideal time/cost-effective strategy to tackle the clinical impact of SARS CoV–2. Thereby, the present study is a promising strategy that proposes the repurposing of approved drugs against pivotal proteins that are responsible for the viral propagation of SARS-CoV-2 virus Angiotensin-converting enzyme-2 (ACE2; 2AJF), 3CL-protease: main protease (6LU7), Papain-like protease (6W9C), Receptor Binding Domain of Spike protein (6VW1), Transmembrane protease serine 2 (TMPRSS-2; 5AFW) and Furin (5MIM) by *in silico* methods. Molecular docking results were analyzed based on the binding energy and active site interactions accomplished with pharmacokinetic analysis. It was observed that both anisomycin and oleandomycin bind to all selected target proteins with good binding energy, achieving the most favorable interactions. Considering the results of binding affinity, pharmacokinetics and toxicity of anisomycin and oleandomycin, it is proposed that they can act as potential drugs against the SARS CoV–2 infection. Further clinical testing of the reported drugs is essential for their use in the treatment of SARS CoV–2 infection.

Introduction

A novel highly pathogenic viral infection from Severe Acute Respiratory Syndrome Coronavirus-2 (SARS-CoV-2) was discovered over a year ago in Wuhan City, Hubei Province, China. On February 11, 2020, the virus was named SARS-CoV-2 by the International Virus Classification Commission (ICTV). Simultaneously, the disease was named by the World Health Organization (WHO) as coronavirus infectious disease 2019 (COVID-19) (1-3). As a human pathogen, SARS-CoV-2 has been declared as a global pandemic by the World WHO based on the rate of increasing spread and the fatality of the viral infection. In comparison to SARS-CoV and MERS-CoV, it was found to be faster transmissible from human-to-human (4-6). Released on March 19, 2021, the confirmed coronavirus cases accounted for more than 122 million and more than 2.7 million deaths. By the 23th of September 2021, the total confirmed cases reached 231 million with more than (4,735,316) total

death around the world. In Saudi Arabia, there are more than (546.792) confirmed cases with more than 8684 deaths (https://www.worldometers.info/coronavirus).

According to the genome sequencing data of SARS-CoV-2, there is more than 82% sequence identity with SARS-CoV and MERS-CoV and >90% sequence identity for essential enzymes and structural proteins, containing genes encoding 3C-like proteinase, RNA-dependent RNA polymerase (RdRp), 20-O-ribose methyltransferase, spike protein, envelope protein, nucleocapsid phosphoprotein, and several unknown proteins (7, 8).To date, there are no approved therapeutic drugs to prevent the expansion of human SARS-CoV-2 and its wide-spreading despite some vaccines which is still in debate and unfavored option for a wide spectrum of people, underling the necessity of an immediate need for antivirals. One of the interesting strategies is to assess their ability to inhibit any SARS-CoV-2 proteins essential for the viral life-cycle. Thereby, four targets including viral ACE2, M^{pro}; PL^{pro}, Receptor Binding Domain of Spike protein and Furin have been chosen. PL^{pro} is crucial in the process of coronavirus replication and infection of the host inducing cleavages of N-terminus of the replicate poly-protein to release Nsp1, Nsp2 and Nsp3, which is essential for enabling virus replication (9, 10). 3CLpro as Nsp5 is essential for the life cycle of the virus (11). RdRp is also known as Nsp12.RdRp is a crucial replicase that catalyzes the synthesis of a complementary viral RNA and thus plays a central role in the replication and transcription of COVID-19 virus genes, possibly with the aid of nsp7 and nsp8 as co-factors (12). Nsp 14 is a nonstructural protein 14 of coronaviruses important for the viral replication and transcription and works as S-adenosyl methionine (SAM)-dependent (guanine-N7) methyl transferase (N7-MTase) (13). The coronavirus main protease (M^{pro}) is considered as the most important target for SARS-CoV-2 drug design that permits the viral gene expression and replication by the proteolytic cleavage of replicase polyproteins, without which the virus replication is severely hampered (14). Currently, although modern medicine is leaning towards the use of phytocompounds produced by plants as secondary metabolites with broad-spectrum activity (15-20), research have been focused also on the repositioning

of existing molecules with therapeutic effect and good availability.

Based on the above facts, target selection and validation are the crucial steps in drug repurposing. Therefore, the main purpose of this work is to test two approved drugs named anisomycin and oleandomycinused as antibiotics for various therapeutic effects. Consequently, anisomycin and oleandomycin will be docket to investigate potential binding-conformation of the ligands of these antibiotics to the binding sites of the SARS-CoV-2 target proteins. Furthermore, as a key step toward unraveling their molecular mechanisms as well as predicting drug side-effects and drug repositioning opportunities, *in silico* target prediction along with their ADMET parameters have been assessed.

Materials and methods

Anisomycin (Figure 1) as an antibiotic, is a translational inhibitor secreted by *Streptomyces* spp., strongly activates the stress-activated mitogen-activated protein (MAP) kinases JNK/SAPK (c-Jun NH2-terminal kinase/stress-activated protein kinase) and p38/RK (also known CSBP for Cytokinin Specific Binding Protein) in mammalian cells, thereby preventing elongation and causing polysome stabilization**.** Oleandomycin (Figure 1) is a macrolide antibiotic synthesized from strains of Streptomyces antibioticus, commercialized under three names and in two forms: as pure oleandomycin ("matromycin," Pfizer; "romicil," Hoffmann-La Roche) and as a mixture with twice its weight of tetracycline ("sigmamycin," Pfizer). The spectrum of activity on micro-organisms is, therefore, wider than that of penicillin and streptomycin.
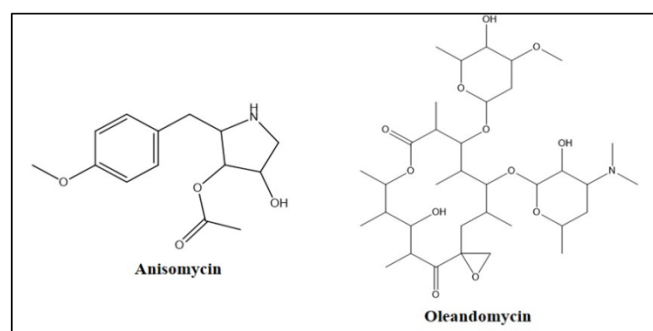

Figure 1. Chemical structure of anisomycin and oleandomycin

Molecular docking

The three-dimensional structure of the target protein was retrieved from RCSB Protein Data Bank (21) with PDB ID:2AJF. Chain A, formed by 597 residues, and bound with ligand "2-acetamido-2-deoxy-beta-D-glucopyranose" in the binding pocket, was considered for docking with selected ligands-Oleandomycin, and Anisomycin. The target protein structure was further analyzed for the presence of domain using NCBI CD Search to search the Conserved Domain Database (22). Docking is based on two major aspects- search algorithm and scoring function. Search algorithms are used to identify the orientation and conformations of the ligand-bound in the binding pocket of the receptor (23). Scoring functions are employed to differentiate between active and random compounds and to predict binding free energies in ligand-protein docking (24). Docking of protein ligands was carried out using AutoDock Vina (19), GOLD (20,21), and LibDock from Discovery Studio Client v20.1.0.19295. The docking softwares used to employ different algorithms to improve binding accuracy. AutoDock Vina uses Broyden-Fletcher-Goldfarb-Shanno algorithm (25). However, GOLD employs a degree of freedom in the binding site that corresponds to the reorientation of hydrogen bond donor and acceptor groups (26-28). The binding affinity and gold fitness scores were obtained from AutoDock Vina and GOLD, respectively for obtaining the best orientation and conformation of the ligands. These values were further correlated with the experimental values. In order to get accurate results, all the docking experiments were performed with the default parameters.

Docking using AutoDock Vina

PDBQT files of receptor protein and ligands were prepared using the Graphical User Interface program AutoDock Tools (ADT). The bound ligand was removed and the grid box was created with size $60 \times 60 \times 60$ XYZ points with a grid spacing of 0.375 Å and grid center was designated at dimensions (x, y, and z): 8.098, 23.137, and 50.858, around the ligand bind site. Protein and ligands were set to rigid during the docking procedure and a configuration file consisting of protein and ligand information along with grid box properties was prepared for executing docking using AutoDock Vina. The ligand pose with

the lowest binding energy/ binding affinity was selected for exploring close intra-molecular interactions with the receptor.

Docking using GOLD (Genetic Optimization for Ligand Docking)

In the GOLD suite, the wizard was used for docking protein and ligands with default parameters. The active site with a 06 Å radius sphere was defined by selecting the bound ligand with in the protein. 10 solutions for each ligand were obtained by applying default Genetic Algorithm settings. The best ligand was selected based on the highest GoldScore fitness function. The ligand and the protein docked complex was further analysed for close intra-molecular interactions.

The molecular docking and visualization studies were also carried out with the help of a commercially available site-features-directed docking (LibDock) program in Discovery Studio (29). The protein 2AJF_A was prepared by adding protein and the binding site was defined by selecting the ligand "2-acetamido-2-deoxy-beta-D-glucopyranose" from the Current selection and defining the xyz coordinates as 7.877869, 23.220714, and 50.836553 with a radius of 10.32 Å. The docking preferences were set to "high quality", and the "Best" Confirmation method with maximum conformations of 255 was selected. The ligand pose with the highest LibDock Score was selected to form docked complex with the receptor for further analysis.

Intra-molecular Interactions in docked complex

Docked complexes of 2AJF_A with Oleandomycin and Anisomycin obtained using AutoDock Vina, GOLD, and LibDock were further analysed for intra-molecular interactions using the View Interaction tool from Discovery Studio Client v20.1.0.19295. Interacting residues of protein and ligand were visualized in 3D and 2D view.

Domain Identification

CD-search revealed the presence of Peptidase_M2 domain, an Angiotensin-converting enzyme, starting from 1 – 588 residues in 2AJF_A.

ADMET prediction

Absorption, Distribution, Metabolism, Excretion and Toxicity predictions were performed for anisomycin and oleandomycin using the pkCSM server (http://biosig.unimelb.edu.au/pkcsm/prediction).

Molecular target predictions

Molecular target predictions are important to find the phenotypical side effects or potential cross-reactivity caused by the action of small biomolecules were obtained by using the web tool (http://www.swisstargetprediction.ch/) and entering the smile formats of the desired drugs to obtain the targets. The prediction concerns the putative targets of the given molecule by utilizing 2D and 3D similarity index with known ligands.

Results and discussion
Molecular docking

In order to found the potential treatment for COVID-19, *in silico* approach has been proposed to validate the repositioning of two drugs such as anisomycin and oleandomycin. Based on the least binding scores, interactions of the selected drugs at the active site of the different SARS-CoV-2-receptors are shown in Figures 2 and 3.

The results depicted in Tables 1 and 2 provided that anisomycin and oleandomycin fit well to the binding site of the selected targets, especially with M^{pro}exhibiting the lowest binding score, -7.62 kcal/mol and -59.72 kcal/mol, respectively.

Docking studies of anisomycin and oleandomycin with the SARS-CoV-2 M^{pro}

SARS-CoV-2 M^{pro}(3C-like proteins) is a cysteine proteases enzyme that can hydrolyze proteins with the help of its Cys-amino acid residues present in the active site and has been proved as the potential target protein to prevent the spread of infection by inhibiting the cleavage of the viral polyprotein.

Our results showed that in the case of anisomycin (Table 1 and Figure 2), The interactions involves between with 6LU7 were Gly143, Ser144, Cys145 (H-bonds), Thr25, Thr26, Leu27, Cys44, Phe140, Leu141, Asn142, His163, His164, Met165, Asp187, Gln189, (van der Waals), Met49 and Cys145(Pi-Sulfur), His41 (Pi-Pi stacked) and Met49, Pro52,

Tyr54 and Arg188 (Alkyl/Pi-Alkyl), meaning that it strongly interacted with the catalytic dyad residues (Cys-145 and His-41) of COVID-19 M^{pro}, as well as interactions with receptor-binding residues of other 20 residues, with sense docking score -47.62 kcal/mol and binding energy kcal/mol. On the other hand, the complex oleandomycin-6LU7 with binding score -59.72 kcal/mol was strongly bound to M^{pro} active site by several interactions withThr24, Thr25, Thr26, Leu27, His41, Met49, Phe140, Leu141, Asn142, Gly143, Ser144, Cys145, His163, His164, Met165, Glu166, His172, Arg182, Gln189 andThr190 residues (Table 2 and Figure 3).

Docking studies of anisomycin and oleandomycin with the SARS-CoV- 2 PL^{pro}

The molecular docking study of anisomycin and oleandomycin compounds with the SARS-CoV-2 PL^{pro}(Table 1 and Figure 2) showed that anisomycin generates the highest docking score cal/mol and binding energy kcal/mol. Whereas, oleandomycin towards SARS-CoV-2 PL^{pro} protein. The binding of anisomycin with PL^{pro}was found to be stabilized by H-bonds with Arg166 and other interactions with Asp164, Val165, Met208, Ser245, Ala246, Glu263, Tyr268, Thr301, Asp302, (van der Waals), Pro248, Tyr273 (C-H bond), Tyr264 (Pi-Stacked), andLeu162 (Pi-Alkyl) residues, while oleandomycin bind to PL^{pro}throughestablishment of-bonds with Tyr273 and several others interactions with Lys157, Glu161, Leu162, Gly163, Asp164, Val165, Arg166, Glu167, Met208, Ser245, Ala246, Pro247, Pro248, Tyr264, Asn267, Tyr268, Thr301, Asp302(Table 2 and Figure 3).

Docking studies of anisomycin and oleandomycin with the SARS-CoV-2 NSP15

The Nonstructural uridylate-specific endoribonuclease named Nsp-15 as an appropriate drug target against SARS-CoV2, essential for its lifecycle and virulence was located in the N terminal domain, leaves 2'-3'-cyclic phosphates 5' to the cleaved bond (https://swissmodel.expasy.org/repository/species/2697049) in which the mechanism of action is independent of the endonuclease activity. Nsp15 affects viral replication by interfering with the host's innate immune response by suppressing the type I IFN

(IFN-α/β, thus eluding detection of viral mRNA by double-stranded RNA sensors. NSP15 is reported to slow viral replication more than any other target (30).

As can be seen from our results (Table 1 and Figure 2), anisomycin fits tightly into the inhibition site of SARS-CoV-2 NSP 15 protein forming one H-bond with Gly 248 and others hydrophobic interactions with His235, Gln245, Leu246, Gly247, Lys290, Val292, Cys293, Ser294, Met331, Thr341, Tyr343 and Pro344 residues, while oleandomycin interacted with Lys90 (H-bond) along with interacting Glu69, Gly165, Val166, Thr167, Ser198, Arg199, Asn200, Leu201, Glu203, Leu252, Leu255, Leu266, Asp268, Pro271, Asp273, Lys277, Tyr279, Val295, Ile296, Asp297 with residues (Table 2 and Figure 3).

Docking studies of anisomycin and oleandomycin with the SARS-CoV-2 Furin

Furin qualified as a target protein for screening of anti-viral compounds is a kind of proprotein convertases enzyme that cycles between the trans-Golgi network and the cell surface, where it recognizes the cleavage motif on protein precursors and converts them to functional proteins through cleavage (31). I was present on the plasma membrane of the host cell may also be playing a very crucial role in the entry of the SARS-CoV-2 virus within cells. The furin recognition site within the SARS-CoV-2 S protein is very similar to that of the highly virulent avian and human influenza viruses suggesting that it may act on S protein during viral production (32).

Regarding to our results, anisomycin occupied the receptor domains with the formation of three C-H bonds with Asp153, Ser253 and Thr365 and one Pi-lone pair with His194 along with several other residues, Arg193, Arg197, Cys198, Leu237, Trp254, Glu255, Asn295, Ser363, His364 and Ser368(Table 1 and Figure 2). Oleandomycin made two H-bond interactions with His194, Asp191 and Asn295, and many hydrophobic interactions with Asp153, Asp154, Arg185, Asn192, Arg193, Leu227, Asp228, Ser253, Trp254, Asp258, Glu255, Pro256, Glu257, and Ser368 residues (Table 2 and Figure 3).

Anisomycin-6VW1

Anisomycin -2AJF

Anisomycin-5MIM

Anisomycin-6W9C

Anisomycin-6LU7   Anisomycin-5AFW

Figure 2. 2D (right) and 3D (left) of Anisomycin with the active site of COVID-19 receptors
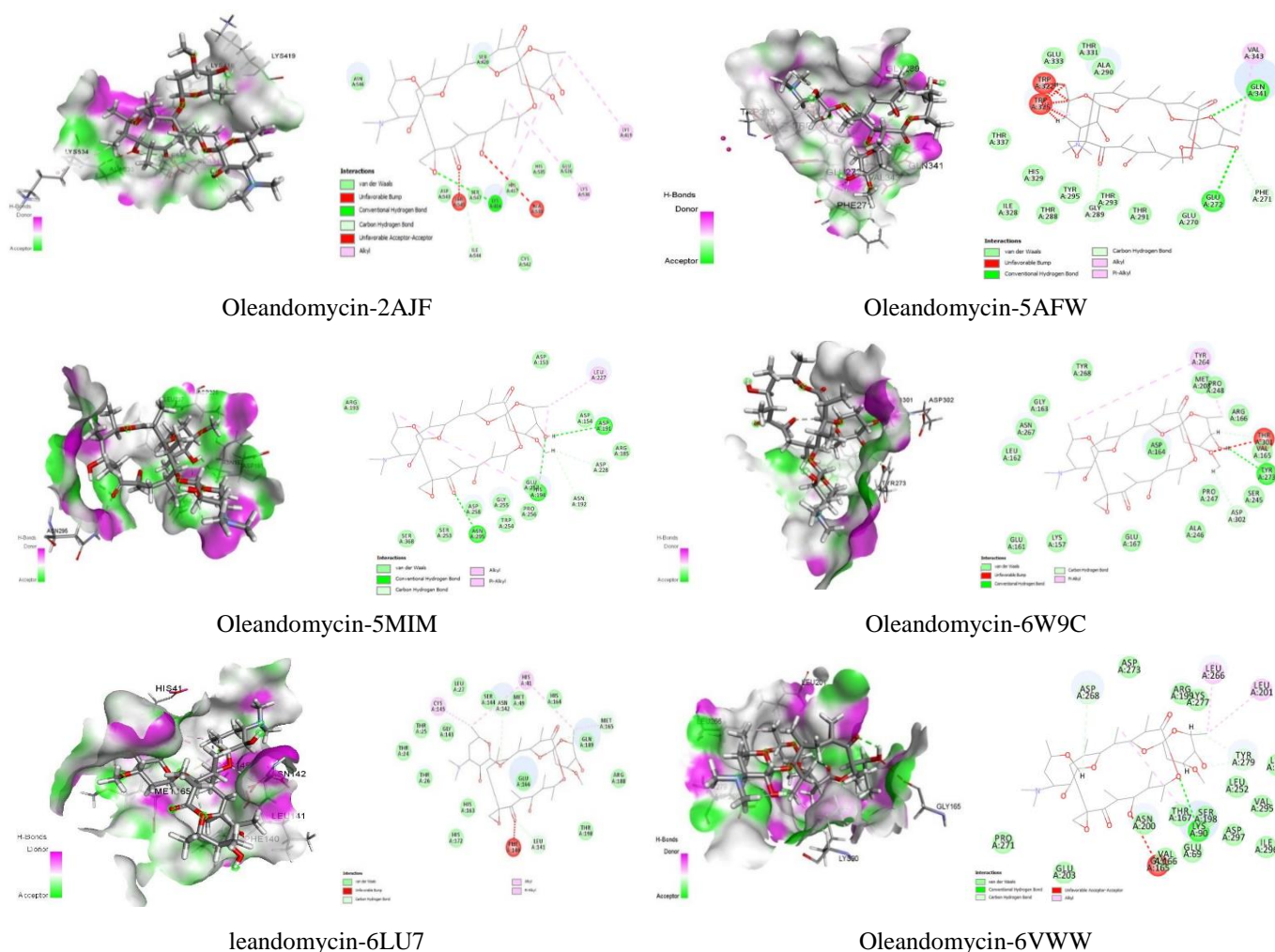

Oleandomycin-2AJF   Oleandomycin-5AFW

Oleandomycin-5MIM   Oleandomycin-6W9C

leandomycin-6LU7   Oleandomycin-6VWW

Figure 3. 2D (right) and 3D (left) of oleandomycin with the active site of COVID-19 receptors

Pharmacokinetics

In order to ensure the drug-likeness properties during the time of preclinical analysis trial in drug discovery and development, assessment of absorption, distribution, metabolism, excretion and toxicity (ADMET) is very crucial for attractive molecules to possess the best chance to become effective drugs (33-38). From the output of some ADMET properties shown in Table 3, it was shown that the liver and intestine cytochrome P450 enzymes (CYP1A2, CYP3A4, CYP2C19, CYP2D6, and CYP2C9) interact with drugs and are responsible for their metabolism. CYP2D6 is responsible for the metabolism of a wide range of compounds in the liver. Its, inhibition by a drug induces the problem of a drug interaction.

Results revealed no inhibition and therefore the lack of any interaction. Anisomycin was found to not act as a P-glycoprotein (P-gp) inhibitor or substrate, however, Oleandomycin was P-g substrate and P-g I inhibitor but not P-g II inhibitor. Their skin permeability was -3.04 and -2.735 units, respectively. They are non-mutagenic and none of them have shown hERG I and hERG II inhibition activity. Their LD 50 values were 2.681and 2.981mol/kg, respectively and their chronic oral rat toxicity (LOAEL) values were 1.109 and 1.722 (log mg/kg_bw/day) without any skin sensitivity. Hence, based on the ADMET analysis, both Anisomycin and Oleandomycin were confirmed to be permissible as available potent drugs with exceptional druglike

properties and therefore they can be further assessed for their *in vitro* SARS-CoV-2 inhibitory activities (Table 3).

Target prediction

Molecular Target studies are important to understand the molecular mechanisms underlying a given phenotype or bioactivity, to rationalize possible side-effects and predict off-targets. An efficient drug will perform its mechanism of action by interacting with the proteins, enzymes and other bio-

macromolecules. Based on their resemblance with known drugs, we can estimate the desired drug targets. The top 50 results of the closely associated receptors based on Target, Common Name, Uniprot ID, ChEMBL-ID, Target Class, Probability and Known actives in 2D/3D were depicted as a pie-chart (Figure 4). As shown, Anisomycin has 13.3% enzyme and 6.7% protease whereas oleandomycin predicts 24% enzyme and 8% protease, as targets.

Table 1. Molecular docking interactions of oleandomycin-receptors

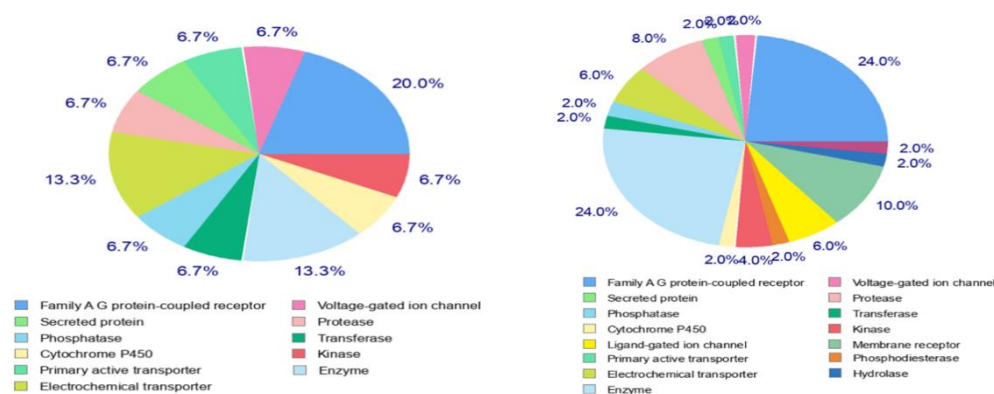| Complex Ligand/Receptor	Interacting residues Receptor *vs.* targets	GOLD Suite (Gold score)	AutoDock Vina score Binding score (kcal/mol)
Anisomycin-6VW1	van der Waals: Pro337, Glu339, Phe342, Asn343, Phe347, Asp364, Leu368, Ser371, Phe373, Trp436; C-H bond: Cys336; Amide-Pi-Stacked: Phe338; Alkyl/Pi-Alkyl: Leu335, Phe338, Val367.	47.41	-6.4
Anisomycin-2AJF	van der Waals: Ala311, Phe314, Ser317, Lys416, Ile421, Asp543, Ile544, Asn546, Ser547; C-H bond:Ser420, Ser545, Glu310; H-bond: Asp177; Unfavorable Donor-Donor: His417; Alkyl/Pi-Alkyl: Lys31, His373, His417.	34.13	-5.9
Anisomycin-5MIM	van der Waals: Arg197, Leu237, Trp254, Glu255, Asn295, Ser363, His364, Ser368, Cys198. Unfavorable Bump: Arg193; C-H bond: Asp153, Ser253, Thr365; Pi-lone pair: His194.	41.86	-7.3
Anisomycin-6W9C	van der Waals: Asp164, Val165, Met208, Ser245, Ala246, Tyr268, Thr301, Asp302, Glu263; H-bond: Arg166; C-H bond: Pro248, Tyr273; Pi-Stacked: Tyr264; Pi-Alkyl: Leu162	44.30	-5.7
Anisomycin-6LU7	van der Waals: Thr25, Thr26, Leu27, Cys44, Leu141, Phe140, Asn142, His163, His164, Met165, Asp187, Gln189; H-bond: Glu143, Ser144, Cys145; Pi-Sulfur: Met49, Cys145; Pi-Pi stacked: His41; Alkyl/Pi-Alkyl: Met49, Pro52, Tyr54, Arg188.	47.62	-5.9
Anisomycin -5AFW	van der Waals: Glu333, Thr337, Gln341, Thr243, Glu272, Glu289, Ala290, Thr331; H-bond: Tyr295, His329; Unvavorable Bump: Trp325, Trp322.	44.60	-5.2
Anisomycin-6VWW	van der Waals: Gln245, Leu246, Lys290, Val292, Cys293, Ser294, Met331, Thr341, Tyr343, Pro344; C-H bond: His235, Gly247, Lys345; H-bond: Gly 248; Alkyl/Pi-Alkyl: Lys345, Leu346.	41.74	-

Figure 4. Pie-chart of top-50 of target predicted for Anisomycin (left) and Oleandomycin (right)

Table 2. Molecular docking interactions of oleandomycin-receptors

Complex Ligand/Receptor	Interacting residues Receptor *vs.* targets	GOLD Suite (Gold score)	AutoDock Vina score Binding score (kcal/mol)
Oleandomycin-6VW1	-	-	-8.8
Oleandomycin-2AJF	van der Waals: His417, Ser420, His535, Glu536, Cys542, Asp543, Asn546, Ser547,; UnvavorableBump/Acceptot-Acceptor:Ala535, Ser545; C-H bond: Lys416; C-H bond: Ile544; Alkyl: Lys416, lys419, Lys534.	36.78	-7.6
Oleandomycin-5MIM	van der Waals: Asp153, Asp154, Arg185, Arg193, Ser253, Trp254, Glu255, Pro256, Glu257, Asp258, Ser368; H-bond: Asp191, His194, Asn295; C-H bond: Asn192, Asp228; Alkyl/Pi-Alkyl: Leu227, Glu257.	39.71	-7.6
Oleandomycin-6W9C	van der Waals: Lys157, Glu161, Leu162, Gly163, Asp164, Val165, Arg166, Glu167, Met208, Ser245, Ala246, Pro247, Pro248, Asn267, Tyr268; H-bond: Tyr273; C-H bond: Asp302; Unfavorable Bump: Thr301; Alkyl: Tyr264	44.94	-6.7
Oleandomycin - 6LU7	van der Waals: Thr24, Thr25, Thr26, Leu27, Met49, Gly143, Ser144, His163, His164, Glu166, His172, Arg182, Gln189, Thr190; C-H bond: Leu141, Asn142, Met165. Unfavorable Bump: Phe140; Alkyl/Pi-Alkyl: His41, Cys145	59.72	-6.3
Oleandomycin-5AFW	van der Waals: Glu270, Thr288, Ala290, Thr291, Thr293, Tyr295, Ile328, His329, Thr331, Glu333, Thr337; H-bond: Glu272, Gln341; C-H bond: Phe271, Glu289; Unfavorable Bump: Trp322, Trp325; Alkyl/Pi-Alkyl: Trp325, Val343.	42.59	-7.7
Oleandomycin-6VWW	van der Waals: Glu69,Val166, Thr167, Ser198, Arg199, Asn200, Glu203, Leu252, Leu255, Pro271, Asp273, Lys277, Tyr279, Val295, Ile296, Asp297; H-bond: Lys90; UnfavorableAceptot-Acceptor: Gly165; C-H bond: Asp268, Tyr279; Alkyl: lys90, Leu201, Leu266.	48.15	-

Table 3. Pharmacokinetics profile of anisomycin and oleandomycin.

	Anisomycin	Oleandomycin		Anisomycin	Oleandomycin
	Absorption			**Distribution**	
Water solubility	-1.417	-4.357	VDss (human)	0.391	0.233
Caco2 permeability	0.471	0.565	Fraction unbound	0.483	0.425
Intestinal absorption	74.969	68.602	BBB permeability	-0.24	-1.433
Skin Permeability	-3.04	-2.735	CNS permeability	-2.871	-3.197
P-g substrate	No	Yes		**Excretion**	
P-g I inhibitor	No	Yes	Total Clearance	0.956	-0.03
P-g II inhibitor	No	No	Renal OCT2 substrate	No	No
	Metabolism			**Toxicity**	
CYP2D6 substrate	No	No	AMES toxicity	No	No
CYP3A4 substrate	No	No	Max. tolerated dose (human)	-0.115	-0.241
CYP1A2 inhibitor	No	No	hERG I inhibitor	No	No
CYP2C19 inhibitor	No	No	hERG II inhibitor	No	No
CYP2C9 inhibitor	No	No	Oral Rat Acute Toxicity (LD50)	2.681	2.981
CYP2D6 inhibitor	No	No	Oral Rat Chronic Toxicity (LOAEL)	1.109	1.722
CYP3A4 inhibitor	No	No	Skin Sensitisation	No	No

Water Solubility =<-4 soluble; Intestinal absorption =below 30 % indicates poor absorbance; Blood-brain barrier Permeability =<-1considered poorly distributed to the brain; CNS (Central Nervous System) permeability =>-2 considered to penetrate the CNS; Total Clearance (logCLtot) =Lower value indicates high drug half lifetime.

Considering the fatality of SARS-CoV-2 and its high infection rate, finding new therapeutic agents, especially drugs is actually a race against time. There is no approved treatment available to eliminate the virus despite the appearance of some vaccines. Docking and scoring software is used widely to enhance the drug design and predict the interaction between drugs and macromolecules in pharmaceutical products. Therefore, SARS-CoV-receptors were used for blinding the docking analysis of some known drugs. As regards toM[pro], its structure comprises three domains, domain 1 (residues 10 to 99), domain 2

(residues 100 to 182) and domain 3 (residues 198 to 303). It is a cysteine protease formed by Cys-145 and His-41 catalytic dyad in its active center which is highly conserved among the coronavirus proteases and plays a major role in substrate binding and the activity of the enzyme. The amino acid residue His-behave as a common acid-base and Cys-is is very well known for its nucleophilic character, exactly responsible for Michael addition reactions to the α, β-unsaturated ketones and nucleophilic attack to the ketones in biological reactions. The proteolytic process is believed to be dependent on the active site cysteine (Cys-145) side chain thiolate nucleophile attack on the amide bond of the substrate (39, 40). The –SH group of Cys145 is ion-paired with His41 forming Cys145-His41 catalytic dyad, which differs from most serine proteases that have a catalytic Ser-His-Asp triad in their active sites (40, 41). Therefore, this protein constitutes an essential opportunity to identify a potential drug candidate as SARS-CoV-2. Consequently, a good SARC-CoV- 2 M ^{pro} inhibitor should contain either conjugated ketone (type-I) or active carbonyls (aldehydes or ketones; type-II) with sufficient hydrophobic parts for non-covalent interactions. PL^{pro} is a multifunctional cysteine protease that processes viral polyproteins to a functional replicase complex leading to viral spread (41). The0 SARS-CoV-2 PL^{pro} shares 83% sequence similarity with SARS-CoV and was involved in deubiquitination, de-ISGylation which obstruct the important signaling pathways causing viral invasion of the innate immune response by the expression of type I interferon (42, 43).

Comparing our results to those of the high-volume pocket of M^{pro} containing Thr24, Thr25, Thr26, Leu27, His41, Cys44, Thr45, Ser46, Met49, Pro52, Tyr54, Phe140, Leu141, Asn142, Gly143, Ser144, Cys145, His163, His164, Met165, Glu166, Leu167, Pro168, His172, Asp187, Arg188, Gln189, Thr190 and Gln192, we found that anisomycin and oleandomycin shared at least 19 common residues. Also, anisomycin and oleandomycin contain at least 15 common residues (Thr24, Thr25, Thr26, Leu27, His41, Met49, Phe140, Leu141, Asn142, Gly143, Ser144, Cys145, His163, His164, Met165) which explain their strongest binding to M^{pro}.

All these characteristics affirm that inhibition of PLpro activity can block the viral replication which

makes it a vital anti-viral drug target. The binding site contained more spacious S3/S4 pockets, rather than the restrictive S1/S2 pockets close to the catalytic residues (44). Our results correlate with the interactions available in the S3/S4 pocket of PL^{pro} containing the following residues, Asp164, Val165, Arg166, Glu167, Met 208, Ala246, Pro247, Pro248, Tyr264, Gly266, Asn267, Tyr268, Gln269, Cys217, Gly271, Tyr273, Thr301 and Asp302 with at least 11 and 14 common amino-acids with Anisomycin and Oleandomycin, respectively.

The crystal structure (PDB ID: 6VWW) for NSP15 showed that His235, Gln245, Gly248, Gln294 Thr341 are the residues of the active site (45). Also, molecular modeling confirms the role of the following residues Thr167; Ile169; Glu171; Ser198; Glu203 and Pro206, in the active pocket. Ser198 *on*e of the important binding residues has been illustrated as essential for recognition (46). These results explain the potential Nsp15 endoribonuclease as a SARS-CoV-2 modulator. Recently, modeling results on NSP15 proved the existence of three binding sites: 1st binding site with the highest pocket score (5.7832) among the three pockets, having twelve amino acids that built up the pocket which are His235, Gln245, Leu246, Gly247, His250, Lys290, Ser294, Val292, Trp333, Thr341, Tyr343 and Pro344. The 2nd binding site was scored at score 4.7232 and made up of the following 18 amino acids Val70, Lys90, Thr196, Ser198, Arg199, Asn200, Leu201, Leu252, Leu266, Asp268, Asp273, Ser274, Thr275, Lys277, Asp297, Met272, Tyr279 and Val295. The 3rd binding site contains Glu45, Asp92, Leu43, Phe44, Trp59, Trp87 and Tyr89. Our results clearly show that anisomycin binds perfectly in the 2nd pocket however oleandomycin with the 1st pocket.

It has been reported that furin may be involved in the proteolytic processing of S protein to make its conformation suitable for binding on ACE2 receptors (46). The priming of SARS-CoV-2 S protein by furin would hypothetically make many more cells susceptible to infection, as compared to S protein priming by TMPRSS-2 alone Furin protease has a binding site from residue 109 to 574, with the presence of catalytic triad Asp153- His194-Ser368 and an additional oxyanion hole at Asn295 (47, 48). Also, it possesses allosteric sites, where inhibitors can bind and change the conformation of the active site.

As shown both anisomycin and oleandomycin confirm the presence of the triad Asp153- His194-Ser368 as well as Asn295 and therefore might be used for prevention and treatment of the COVID19. Pharmacokinetic studies will be beneficial for scientists to search out safe and effective drug candidates in the initial stage of drug discovery. Based on the aforementioned results, the drug-likeness of anisomycin and oleandomycin have been validated. Also, they were predicted to be good inhibitors of the SARS-CoV proteins and could be propitious as therapeutics for SARS-CoV-2 infection.

Funding

Acknowledgments

Conflict of Interest

The authors declare no conflict of interest.

References

1. Gorbalenya AE, Baker SC, Baric RS, de Groot RJ, Drosten C, Gulyaeva AA, Haagmans BL, Lauber C, Leontovich AM, Neuman BW, Penzar D, Perlman S, Poon LLM, Samborskiy D, Sidorov IA, Sola I, Ziebuhr J. Severe acute respiratory syndrome-related coronavirus: the species and its viruses–a statement of the Coronavirus Study Group. *bioRxiv* 2020; doi: https://doi.org/10.1101/2020.02.07.937862.

2. Bonilla-Aldana DK, Dhama K, Rodriguez-Morales AJ. Revisiting the one health approach in the context of COVID-19: a look into the ecology of this emerging disease. Adv Anim Vet Sci 2020;8(3):234-237.

3. Rabaan AA, Al-Ahmed SH, Sah R, Tiwari R, Yatoo MI, Patel SK, Pathak M, Malik YS, Dhama K, Singh KP, Bonilla-Aldana DK, Haque S, Martinez-Pulgarin DF, Rodriguez-Morales AJ, Leblebicioglu H. SARS-CoV-2/COVID-19 and advances in developing potential therapeutics and vaccines to counter this emerging pandemic. Ann Clin Microbiol Antimicrob 2020;19(1):40.

4. Krishnaprasad B, Swastika M, Chetan HM, Akhil S, Usha YNC, Yogendra N SARS-CoV-2 entry inhibitors by dual targeting TMPRSS-2 and ACE2: An *in silico* drug repurosing study. Eur J Pharmacol 2021;896:173922.

5. Fani M, Teimoori A, Ghafari S. Comparison of the COVID-2019 (SARS-CoV-2) pathogenesis with SARS-CoV and MERS-CoV infections. Future Virol 2020;15(5):317-323.

6. Wang C, Horby PW, Hayden FG, Gao GF. A novel coronavirus outbreak of global health concern. Lancet 2020;395(10223):470473.

7. Romano M, Ruggiero A, Squeglia F, Maga G, Berisio R. A Structural View of SARS-CoV-2 RNA Replication Machinery: RNA Synthesis, Proofreading and Final Capping. Cells 2020;9(5):1267.

8. Aftab SO, Ghouri MZ, Massoud MU, Haider Z, Khan Z, Munawar N. Analysis of SARS-CoV-2 RNA-dependent RNA polymerase as a potential therapeutic drug target using a computational approach. J Transl Med 2020;18:275.

9. Wu C, Liu Y, Yang Y, Zhang P, Zhong W, Wang Y, Wang Q, Xu Y, Li M, Li X, Zheng M, Chen L, Li H. Analysis of therapeutic targets for SARS-CoV-2 and discovery of potential drugs by computational methods. Acta Pharm Sin B 2020;10(5):766-788.

10. Wong NA, Saier SH. The SARS-Coronavirus Infection Cycle: A Survey of Viral Membrane Proteins, Their Functional Interactions and Pathogenesis. Int J Mol Sci 2021;22(3):1308.

11. Ju X , Zhu Y, Wang Y , Li J, Zhang J , Gong M , Ren W , Li S , Zhong J, Zhang QC, Zhang R, Ding Q. A novel cell culture system modeling the SARS-CoV-2 life cycle. bioRxiv 2020. 12.13.422469.

12. Gao Y, Yan L, Huang Y, Liu F, Zhao Y, Cao L, Wang T, Sun Q, Ming Z, Zhang L, Ge J, Zheng L, Zhang Y, Wang H, Zhu Y, Zhu C, Hu T, Hua T, Zhang B, Yang X, Li J, Yang H, Liu Z, Xu W, Guddat LW, Wang Q, Lou Z, Rao Z. Structure of the RNA-dependent RNA polymerase from COVID-19 virus. Science 2020; 368(6492):779-782.

13. Saramago M, Bárria C, Costa V, Souza CS, Viegas SC, Domingues S, Lousa D, Soares CM, Arraiano CM, Matos RG. New targets for

drug design: Importance of nsp14/nsp10 complex formation for the 3'-5' exoribonucleolytic activity on SARS-CoV-2. *bioRxiv* 2021.01.07.425745.

14. Roe MK, Junod NA, Young AR, Beachboard DC, Stobart CC. Targeting novel structural and functional features of coronavirus protease nsp5 (3CL^pro, M^pro) in the age of COVID-19. J Gen Virol 2021: doi.org/10.1099/jgv.0.001558.

15. Mseddi K, Alimi F, Noumi E, Veettil VN, Deshpande S, Adnan M, Hamdi A, Elkahoui S, Alghamdi A, Kadri A, Patel M, Snoussi M. *Thymus musilii* Velen. as a promising source of potent bioactive compounds with its pharmacological properties: *In vitro* and *in silico* analysis. Arab J Chem 2020;13:6782-6801.

16. Felhi S, Hajlaoui H, Ncir M, Bakari S, Ktari N, Saoudi M, Gharsallah N, Kadri A. Nutritional, phytochemical and antioxidant evaluation and FT-IR analysis of freeze-dried extracts of *Ecballium elaterium* fruit juice from three localities. J Food Sci Technol 2016;36:646-655.

17. Daoud A, Ben Mefteh F, Mnafgui K, Turki M, Jmal S, Ben Amar R, Ayadi F, ElFeki A, Abid L, Rateb ME, Belbahri L, Kadri A, Gharsallah N. Cardiopreventive effect of ethanolic extract of date palm pollen against isoproterenol induced myocardial infarction in rats through the inhibition of the angiotensin-converting enzyme. Exp Toxicol Pathol 2017;69:656-665.

18. Felhi S, Saoudi M, Daoud A, Hajlaoui H, Ncir M, Chaabane R, El Feki A, Gharsallah N, Kadri A. Investigation of phytochemical contents, *in vitro* antioxidant and antibacterial behavior and *in vivo* anti-inflammatory potential of *Ecballium elaterium* methanol fruits ex-tract. Food Sci Technol (Campinas) 2017;37:558-563.

19. Bakari S, Hajlaoui H, Daoud A, Mighri H, Ross-Garcia JM, Gharsallah N, Kadri A. Phytochemicals, antioxidant and antimicrobial potentials and LC-MS analysis of hydroalcoholic extracts of leaves and flowers of *Erodium glaucophyllum* collected from Tunisian Sahara. Food Sci Biotechnol 2018;38(2):310–317.

20. Alminderej F, Bakari S, Almundarij TI, Snoussi M, Aouadi K, Kadri A. Antimicrobial and wound healing potential of a new chemotype from *Piper cubeba* L. essential oil and *in silico* study on *S. aureus* tyrosyl-tRNA synthetase protein. Plants 2021;10:205-224.

21. Berman H, Henrick K, Nakamura H. Announcing the worldwide Protein Data Bank. Nat Struct Biol 2003;10(12): 980.

22. Lu S, Wang J, Chitsaz F, Derbyshire MK, Geer RC, Gonzales NR, et al. CDD/SPARCLE: the conserved domain database in 2020. Nucleic Acids Res 2020;48(D1):D265-D268.

23. Sousa SF, Fernandes PA, Ramos MJ. Protein-ligand docking: current status and future challenges. *Proteins* 2006;65(1):15-26.

24. Bissantz C, Folkers G, Rognan D. Protein-based virtual screening of chemical databases. 1. Evaluation of different docking/scoring combinations. J Med Chem 2000; 43(25):4759-4767.

25. Trott O, Olson AJ. AutoDock Vina: improving the speed and accuracy of docking with a new scoring function, efficient optimization, and multithreading. J Comput Chem 2010;31(2):455-461.

26. Jones G, Willett P, Glen RC. Molecular recognition of receptor sites using a genetic algorithm with a description of desolvation. J Mol Biol 1995;245(1): 43-53.

27. Jones G, Willett P, Glen R C, Leach AR, Taylor R. Development and validation of a genetic algorithm for flexible docking. J Mol Biol 1997;267(3):727-748.

28. Meng XY, Zhang HX, Mezei M, Cui, M. Molecular docking: a powerful approach for structure-based drug discovery. Curr Comput Aided Drug Des 2001;7(2):146-157.

29. Saeed M, Saeed A, Alam M-J, Alreshidi M. Computational hunting of natural active compounds as an alternative for Remdesivir to target RNA-dependent polymerase. Cell Mol Biol 2021;67(1):45-49.

30. Hackbart M, Deng X, Baker S-C. Coronavirus endoribonuclease targets viral polyuridine sequences to evade activating host sensors. Proc Natl Acad Sci USA 2020;117(14): 8094-8103.

31. Braun E, Sauter D. Furin-mediated protein processing in infectious diseases and cancer. Clin Transl Immunology 2019;8(8):e1073.

32. Andersen KG, Rambaut A, Lipkin WI, Holmes EC, Garry RF. The proximal origin of SARS-CoV-2. Nat Med 2020;26(4):450–452.

33. Othman IMM, Gad-Elkareem MAM, Anouar EH, Aouadi K, Kadri A, Snoussi M. Design, synthesis ADMET and molecular docking of new imidazo[4,5-b]pyridine-5-thione derivatives as potential tyrosyl-tRNA synthetase inhibitors. Bioorg Chem 2020;102:104105.

34. Othman IMM, Gad-Elkareem MAM, Anouar EH, Snoussi M, Aouadi K, Kadri A. Novel fused pyridine derivatives containing pyrimidine moiety as prospective tyrosyl-tRNA synthetase inhibitors: Design, synthesis, pharmacokinetics and molecular docking studies. J Mol Struct 2020;1219:128651.

35. Ghannay S, Bakari S, Msaddek M, Vidal S, Kadri A, Aouadi K. Design, synthesis, molecular properties and in vitro antioxidant and antibacterial potential of novel enantiopure isoxazolidine derivatives. Arab J Chem 2020;13:2121-2131.

36. Kadri A, Aouadi K. *In vitro* antimicrobial and α-glucosidase inhibitory potential of enantiopure cycloalkylglycine derivatives: Insights into their in silico pharmacokinetic, druglikeness, and medicinal chemistry properties. J Appl Pharm Sci 2020;10:107-115.

37. Snoussi M, Redissi A, Mosbah A, De Feo V, Adnan M, Aouadi K, Alreshidi M, Patel M, Kadri A, Noumi E. Emetine, a potent alkaloid for the treatment of SARS-CoV-2 targeting papain-like protease and non-structural proteins: pharmacokinetics, molecular docking and dynamic studies. J Biomol Struct Dyn 2021; DOI: 101080/0739110220211946715

38. Alminderej F, Bakari S, Almundarij TI, Snoussi M, Aouadi K, Kadri A. Antioxidant activities of a new chemotype of *Piper cubeba* L. fruit essential oil (methyleugenol/eugenol): *In silico* molecular docking and ADMET studies. Plants 2020;9:1534.

39. Sepay N, Sekar A, Halder UC, Alarifi A, Afzal M. Anti-COVID-19 terpenoid from marine sources: A docking, ADMET and molecular dynamics study. J Mol Struct 2021;1228:129433.

40. Ullrich S, Nitsche C. The SARS-CoV-2 main protease as drug target. Bioorg Med Chem Lett 2020;30(17):127377.

41. Jin Z, Du X, Xu Y, Deng Y, Liu M, Zhao Y, Zhang B, Li X, Zhang L, Peng C, Duan Y, Yu J, Wang L, Yang K, Liu F, Jiang R, Yang X, You T, Liu X, Yang X., Bai F, Liu H, X. Liu, Guddat LW, Xu W, Xiao G, Qin C, Shi Z, Jiang H, Rao Z, Yang H. Structure of Mpro from SARS-CoV-2 and discovery of its inhibitors. Nature 2020;582:289-293.

42. Gao X, Qin B, Chen P, Zhu K, Hou P, Wojdyla JA, Wang M, Cui S Crystal structure of SARS-CoV-2 papain-like protease. Acta Pharm Sin B 2021;11(1):237-245.

43. B´aez-Santos M, John SES, Mesecar AD. The SARS-coronavirus papain-like protease: structure, function and inhibition by designed antiviral compounds. Antivir Res 2015;115: 21-38.

44. Rahman F, Tabrez S, Ali R, Alqahtani AS, Ahmed MZ, Rub A. Molecular docking analysis of rutin reveals possible inhibition of SARS-CoV-2 vital proteins. J Tradit Complement Med 2021;11(2):173-179.

45. Pal S, Talukdar DA. Compilation of Potential Protein Targets for SARS-CoV-2: Preparation of Homology Model and Active Site Determination for Future Rational Antiviral Design. ChemRxiv 2020:https://doi.org/10.26434/chemrxiv.12084468.v1

46. Chambers JP, Yu J, Valdes JJ, Arulanandam BP. SARS-CoV-2, Early Entry Events. J Pathog 2020; 9238696. doi: 10.1155/2020/92386962020;24:9238696.

47. Ercisli M., Lechun, G, Azeez S, Hamasalih R, Song S, Aziziaram Z. Relevance of genetic polymorphisms of the human cytochrome P450 3A4 in rivaroxaban-treated patients. Cell Mol Biomed Rep 2021; 1(1): 33-41.

48. Dahms SO, Arciniega M, Steinmetzer T, Huber R, Than ME. Structure of the unliganded form of the proprotein convertase furin suggests activation by a substrate-induced mechanism. Proc Natl Acad Sci USA 2016;113(40):11196-11201.